Article:
Stull, F, Koldewey, P, Humes, JR orcid.org/0000-0002-1407-7880 et al. (2 more authors) (2016) Substrate protein folds while it is bound to the ATP-independent chaperone Spy. Nature Structural & Molecular Biology, 23 (1). pp. 53-58. ISSN 1545-9993

https://doi.org/10.1038/nsmb.3133

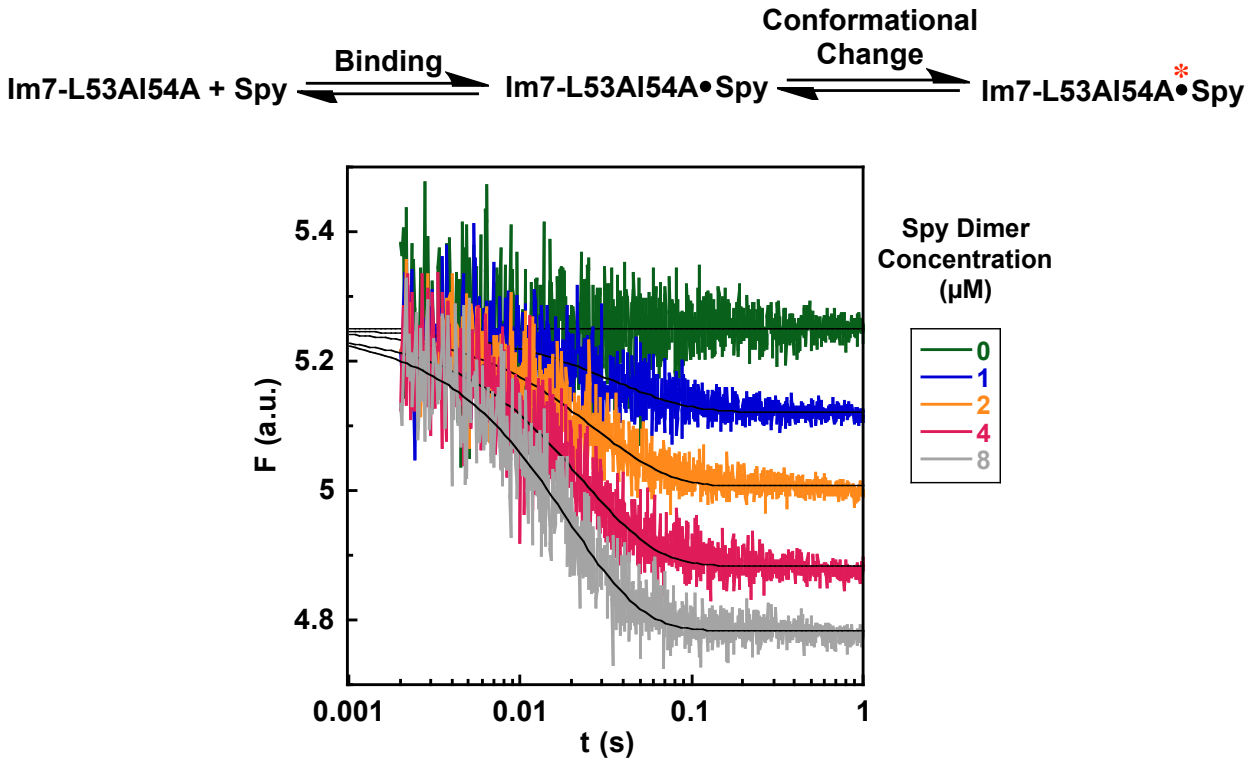

Supplementary Figure 1. Binding of Spy to Im7-L53AI54A ($Im7_l$). (**Top**) A two-step kinetic mechanism where Spy first binds Im7-L53AI54A followed by a conformational change within the complex (denoted by the red asterisk). The hyperbolically increasing dependence of k_{obs} on Spy concentration when Spy binds Im7-L53AI54A (**Fig. 3b**, main text) is consistent with this mechanism, in which the fluorescence decrease reflects the conformational change within the complex. The plot of k_{obs} versus Spy concentration is hyperbolic in part because k_{obs} depends on the fractional concentration of the Im7-L53AI54A-Spy complex prior to the conformational change[1,2], which changes with Spy concentration based on the K_d for the initial binding step. (**Bottom**) Overlay of traces for Spy binding Im7-L53AI54A at different Spy concentrations. The traces at all Spy concentrations extrapolate back to the fluorescence of Im7-L53AI54A alone at time zero, indicating that there is no burst phase and that no fluorescence change occurs with the initial binding step.

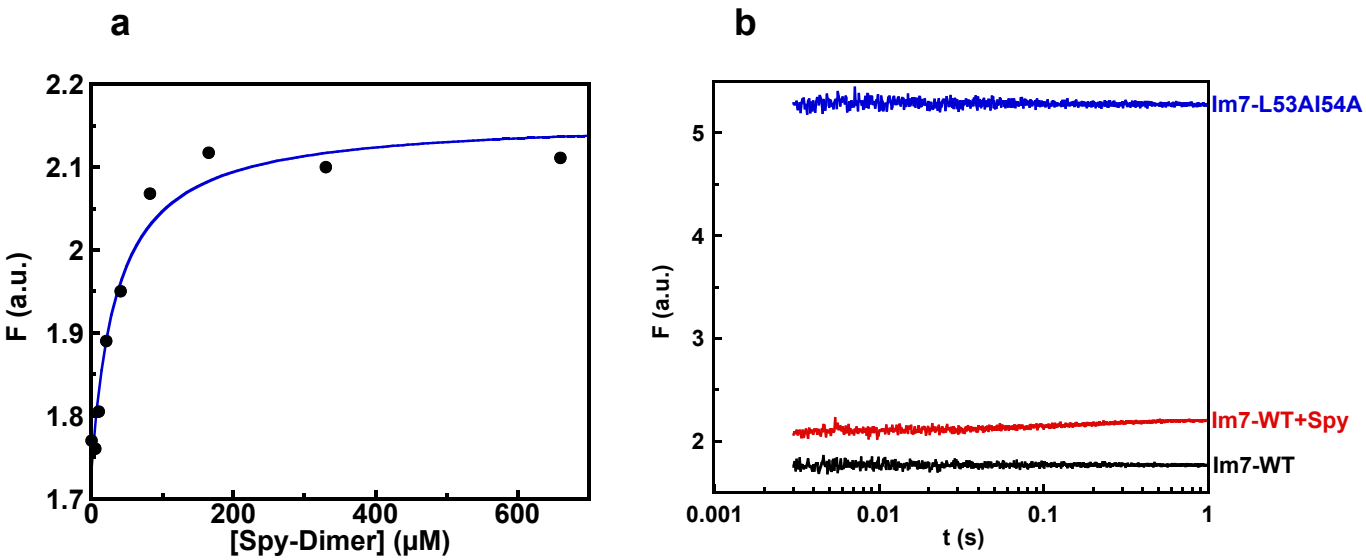

Supplementary Figure 2. Burst phase when Spy binds native Im7 and relative fluorescence intensity of Im7-WT:Spy complex. (**a**) Burst phase size when Spy binds 4.8 μM native Im7-WT at different Spy concentrations. The initial fluorescence observable by stopped-flow when Spy binds native Im7-WT is higher than the fluorescence of Im7-WT alone (**Fig. 4a**, main text). The plot in **a** shows the fluorescence extrapolated to time zero for each trace at different Spy concentrations. The amplitude of this burst phase reaches a saturating level at high Spy concentrations, consistent with Spy binding native Im7 within the dead time of the stopped-flow instrument. The blue line is the fit to a square hyperbola, which gives a half-saturation concentration of 36 ± 11 μM. (**b**) A comparison of the change in tryptophan fluorescence when Spy binds native Im7-WT with the fluorescence of $Im7_I$. The tryptophan fluorescence of Im7-WT bound to saturating concentrations of Spy (red) is higher than the fluorescence of Im7-WT alone (black). The amplitude of the post burst phase increase in fluorescence when Spy binds Im7-WT is 0.1 fluorescence units, which is ~3% of the total fluorescence intensity difference between the $Im7_I$ mimic, Im7-L53AI54A, and Im7-WT (3.5 fluorescence units), evidence that only ~3% of Im7-WT becomes unfolded to $Im7_I$ in the Im7-Spy complex. This is consistent with the change in equilibrium constant for the $Im7_I$-$Im7_N$ step expected from the difference in affinities of Spy for $Im7_I$ and $Im7_N$: the equilibrium constant for the unbound $Im7_I$-$Im7_N$ step (K_{IN}) is 319 in 0.7 M urea (**Supplementary Fig. 5**), which means that 99% of the Im7 is in the native state prior to binding Spy; Spy binds $Im7_I$ with ~6-fold higher affinity than $Im7_N$, making the $Im7_I$-$Im7_N$ equilibrium constant 53 in 0.7 M urea when bound to Spy; this means that 98% of the Im7-WT should be in the native state when bound to Spy, and that ~1% of $Im7_N$ should unfold to $Im7_I$ upon binding Spy.

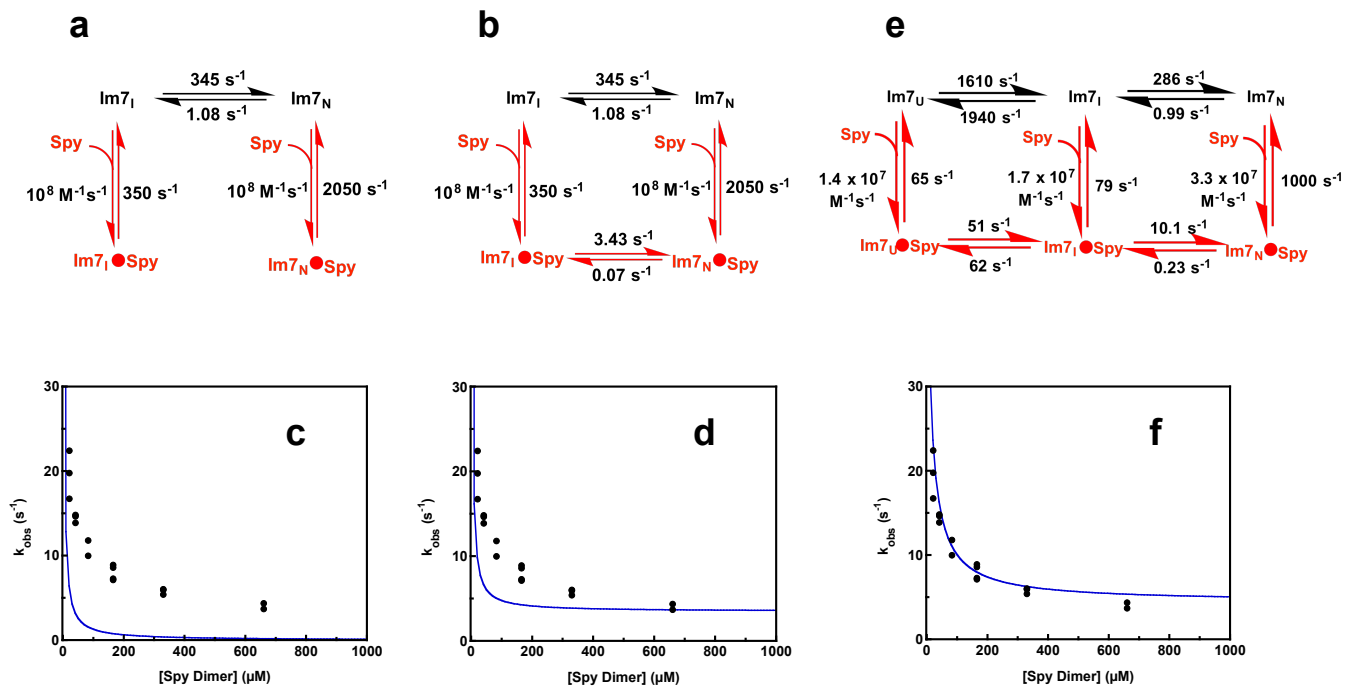

Supplementary Figure 3. Im7-WT partially unfolds while bound to Spy. The decreasing dependence of k_{obs} on Spy concentration of the post-burst phase step (**Fig. 3c**) indicates that Spy induces the unfolding of a small proportion of the $Im7_N$ in Im7-WT into $Im7_I$. In addition, the burst phase seen when Spy binds Im7-WT (**Fig. 4a**) confirms that Spy is capable of binding $Im7_N$. These two points on their own do not address whether Im7 must be released from Spy for the partial unfolding of Im7-WT to occur (**a**), or if Im7 can be directly unfolded while in complex with Spy (**b**). (**c**,**d**) The simulated dependence of k_{obs} on Spy concentration for the mechanisms shown in **a** and **b**, respectively. The simulated dependence of k_{obs} on Spy concentration is shown as a blue line and the black points are the experimental k_{obs} values from **Fig. 3c**, main text. The simulated dependence of k_{obs} on Spy concentration for the mechanism *omitting* folding/unfolding of Im7 while bound (**c**) shows that k_{obs} should reach 0 s^{-1} at high Spy concentrations. However, the simulated dependence of k_{obs} on Spy concentration for the mechanism *allowing* folding/unfolding of Im7 while bound (**d**) shows that k_{obs} should approach the sum of the folding and unfolding rate constants while bound at high Spy concentrations (in this case, 3.5 s^{-1}). The trend in **d** clearly matches the trend of the observed data better than in **c**, suggesting that the partial unfolding of Im7-WT by binding to Spy occurs *while bound* to the chaperone. The difference in the half-saturation concentration between the simulated and experimental data in **d** is due to the mechanism **c** being an oversimplification of the complete mechanism, since $Im7_I$ is also in equilibrium with $Im7_U$. If the complete mechanism (**e**) is used with the rate constants obtained by global analysis (**Table 1** and **Supplementary Fig. 7**), there is excellent agreement between the observed and simulated data (**f**).

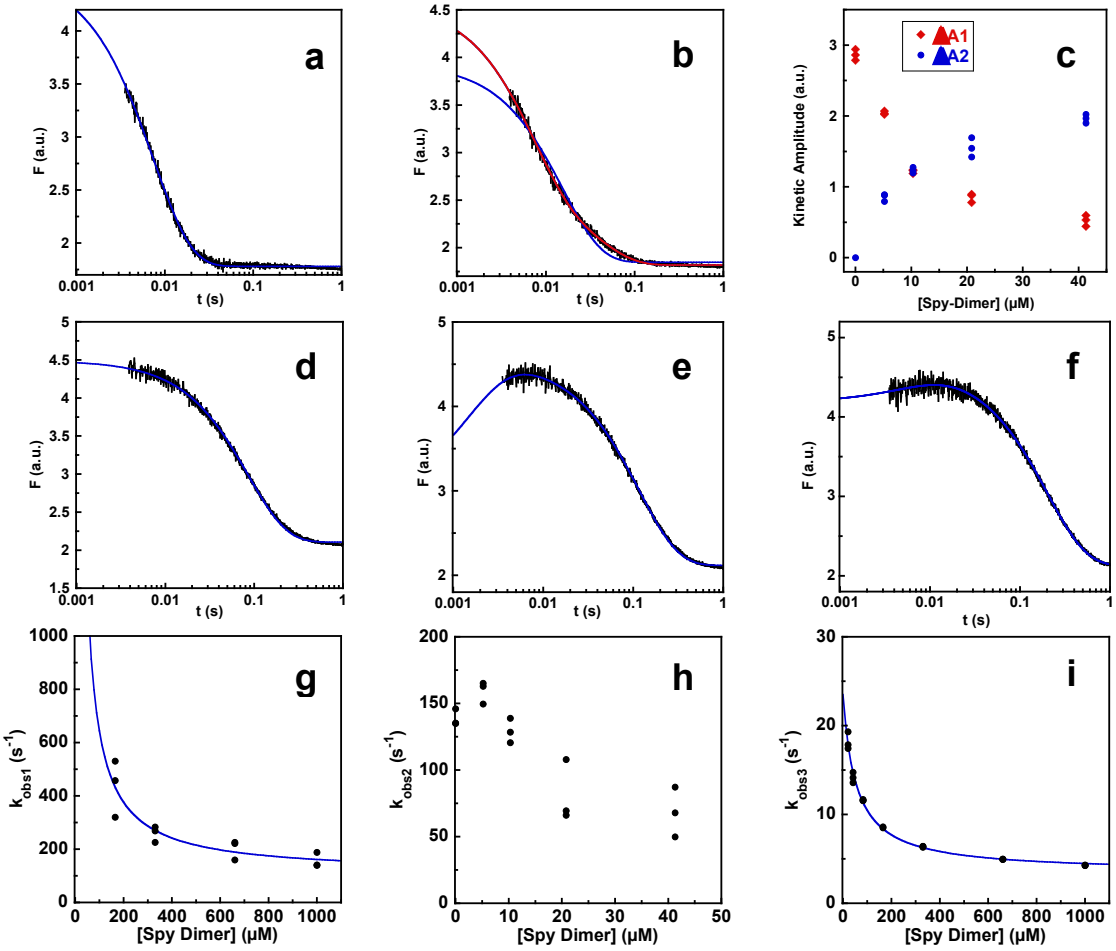

Supplementary Figure 4. Primary analysis of stopped-flow traces of Im7 folding in the presence of Spy. (**a**) 4.8 μM Im7 folding in the absence of Spy. The trace can be fitted with a single exponential (blue line). (**b**) 4.8 μM Im7 folding in the presence of 5 μM Spy dimer. The trace cannot be adequately fitted with a single exponential (blue line), but can be fitted with a double exponential function (red line). (**c**) Kinetic amplitudes for the two phases detectable at low Spy concentrations (corresponding to k_{obs1} and k_{obs2} in **g** and **h**). The amplitude for the first phase (ΔA1) decreases with increasing Spy concentration, whereas the amplitude for the second phase (ΔA2) increases. ΔA1 decreases to the point where traces with ≥83 μM Spy can be fit with a single exponential. (**d**) 4.8 μM Im7 folding in the presence of 83 μM Spy dimer. The trace can be fitted with a single exponential (blue line). (**e**,**f**) 4.8 μM Im7 folding in the presence of 165 and 660 μM Spy dimer, respectively. Traces with ≥165 μM Spy showed an increase in fluorescence in the first 20 msec, which is likely the conversion of $Im7_U$ to $Im7_I$ that only becomes detectable at high Spy concentrations. As a result, transients at these concentrations had to be fitted to a double exponential function (blue line). (**g**) Dependence of the observed rate constant on Spy concentration for the increase in fluorescence detectable only at the highest Spy concentrations (k_{obs1}). k_{obs1} decreased with Spy concentration, reaching a limit of ~110 s^{-1}. (**h**) Observed rate constant for the first decreasing fluorescence phase detectable only at low Spy concentrations (k_{obs2}). At higher Spy concentrations, the amplitude of this phase is too small to fit accurately. (**i**) Observed rate constant for the slow decreasing fluorescence phase detectable at all Spy concentrations (k_{obs3}). k_{obs3} decreases with increasing Spy concentration, reaching a limit of 3.5 ± 0.3 s^{-1}. k_{obs3} is indistinguishable from the observed rate constant for Spy binding to Im7-WT under native conditions (**Fig. 3c**), suggesting that both exponentials are monitoring the same step in the kinetic mechanism.

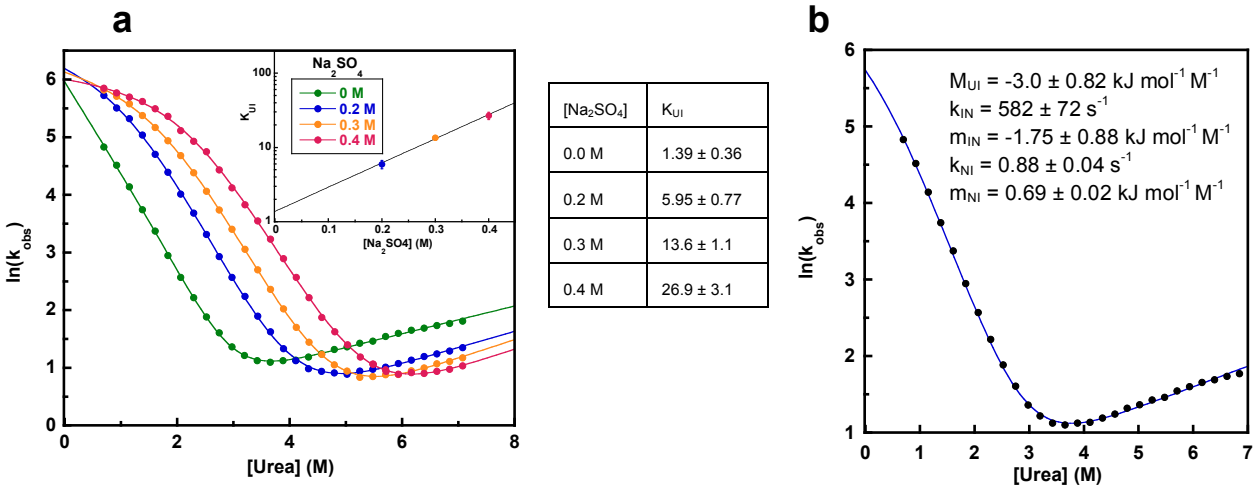

[Na_2SO_4]	K_{UI}
0.0 M	1.39 ± 0.36
0.2 M	5.95 ± 0.77
0.3 M	13.6 ± 1.1
0.4 M	26.9 ± 3.1

Supplementary Figure 5. Folding and unfolding data for Im7-WT in the absence of Spy. (**a**) Sulphate extrapolation of Im7-WT folding and unfolding to determine the equilibrium constant for the conversion of unbound $Im7_U$ to unbound $Im7_I$ (K_{UI}). Initially, the K_{UI} value was poorly defined for Im7 folding/unfolding in 40 mM HEPES-KOH, pH 7.5, 100 mM NaCl, 10°C because the folding intermediate is relatively unstable under those conditions, which produces very little curvature in the folding arm of the chevron plot. To better define K_{UI} under our standard conditions, we collected data for Im7 folding and unfolding at several concentrations of Na_2SO_4, which stabilizes the folding intermediate of Im7. The inset shows the sulphate dependence of K_{UI}. Extrapolation back to 0 M Na_2SO_4 indicates that K_{UI} is 1.39 ± 0.36 in 40 mM HEPES-KOH, pH 7.5, 100 mM NaCl, 10°C. (**b**) The denaturant dependence of Im7 folding and unfolding kinetics in 40 mM HEPES-KOH, pH 7.5, 100 mM NaCl, 10°C fitted with a K_{UI} value of 1.39. A good fit was obtained when K_{UI} was fixed at 1.39. The values for K_{UI}, k_{IN}, and k_{NI} in 0.7 M urea (the urea concentration in the experiments used for global fitting, **Supplementary Fig. 6**) were calculated using the relationship $k_{xy} = k_{xy}^{H2O} e^{(m_{xy}/RT)[Urea]}$.[3] Calculated in this way, the values in 0.7 M urea are K_{UI} = 0.57 ± 0.29, k_{IN} = 345 ± 56 s^{-1} and k_{NI} = 1.08 ± 0.04 s^{-1}.

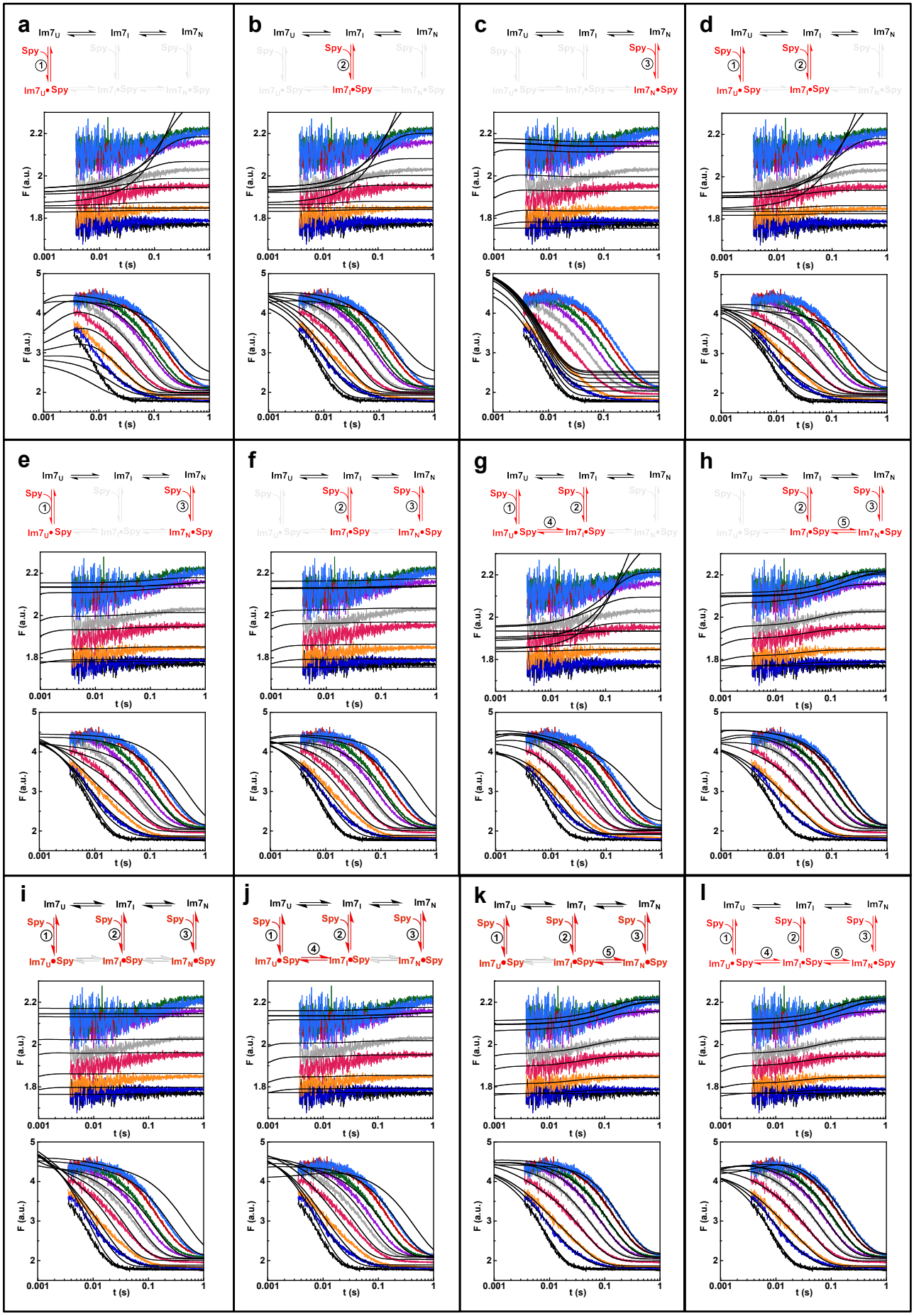
a
b
c
d
e
f
g
h
i
j
k
l
Im7U
Im7I
Im7N
Spy
Im7U•Spy
Im7I•Spy
Im7N•Spy
F (a.u.)
t (s)

Supplementary Figure 6. Global fitting to various kinetic mechanisms. In all 12 panels (**a-l**), top: mechanism used in globally fitting the two following plots; middle: global fitting of Spy binding Im7-WT traces; bottom: global fitting of Im7 folding in the presence of Spy traces. The Spy concentrations range from 0 μM (black trace) to 660 μM (light blue trace). The black lines in the plots are the best fit to the data. Although the mechanisms in **h** and **k** superficially appear to fit the data, they fail to account for the initial increase in fluorescence in the first 20 ms of the traces for Im7 folding in the presence of the highest Spy concentrations (light blue trace). Only the kinetic mechanism that allows complete folding of Im7 while bound to Spy (**l**) can fit the data for Spy binding Im7-WT as well as the initial fluorescence increase and the subsequent fluorescence decrease observed when Im7 folds in the presence of Spy.

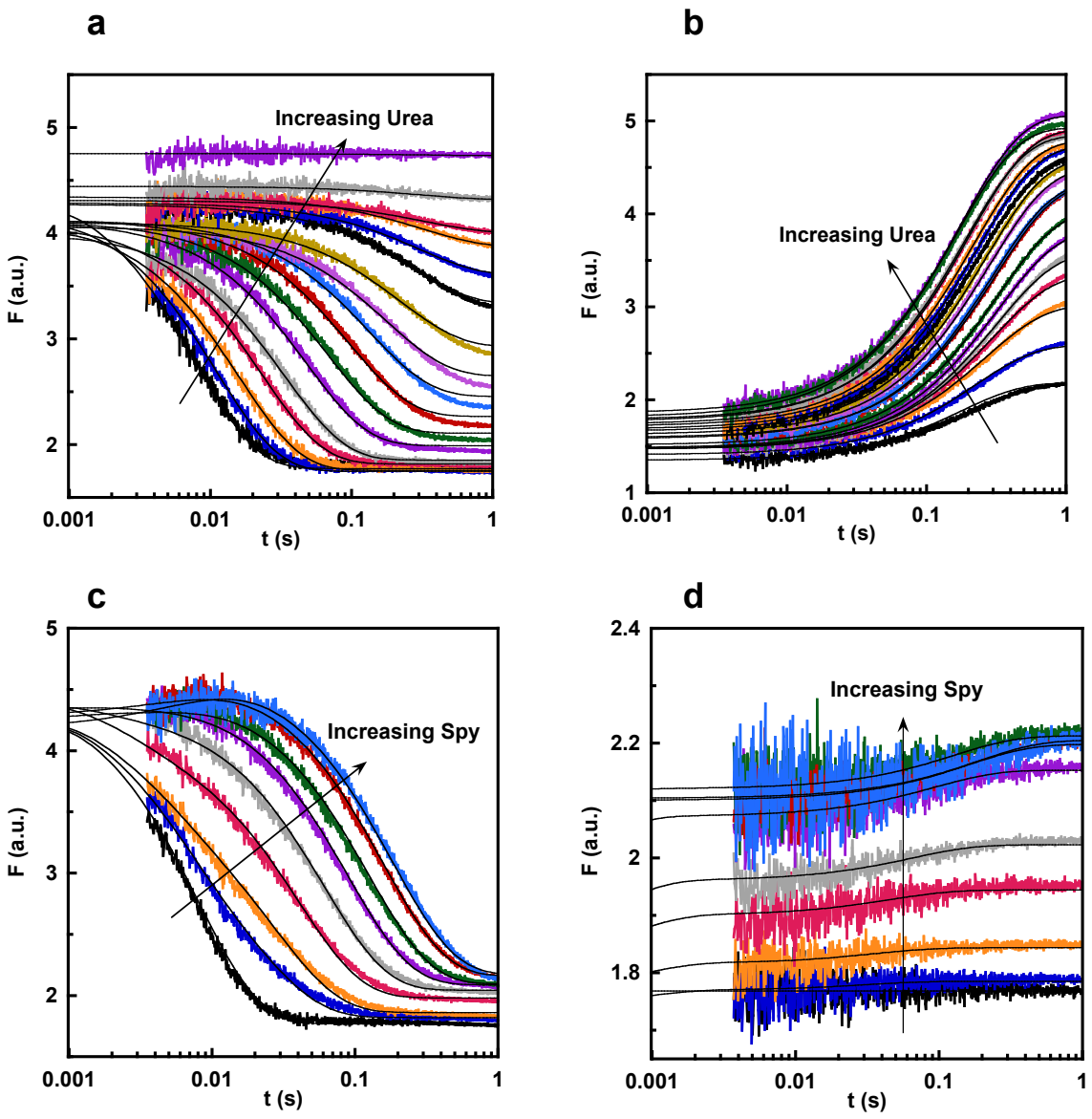

Supplementary Figure 7. Simultaneous fitting of fluorescence transients for all data to the mechanism that allows complete folding of Im7 while bound to Spy. (**a**) and (**b**), Fluorescence transients for Im7 folding and unfolding, respectively, at different urea concentrations in the absence of Spy. (**c**) Fluorescence transients for Im7 folding in the presence of different Spy concentrations in 0.7 M urea. (**d**) Fluorescence transients for Spy binding to Im7-WT at different Spy concentrations in 0.7 M urea. The black lines in all plots are the best fit to the data. The goodness of fit (X^2/Degrees of freedom) was 1.49. Data were collected in 40 mM HEPES-KOH, pH 7.5, 100 mM NaCl at 10°C. The rate constants and fluorescence scaling factors obtained from the global analysis can be found in **Table 1** of the main text and **Supplementary Table 1**.

Supplementary Table 1 Comparison of parameters obtained from the global fitting with those obtained from the Im7 mutants that mimic the Im7 folding pathway states

	Values from global fitting of kinetic data			Values from Im7 mimic mutants		
	$Im7_U$	$Im7_I$	$Im7_N$	Im7-L18AL19AL37A[a]	Im7-L53AI54A[b]	Im7-WT
K_d (μM)	4.7 ± 1.1	4.7 ± 0.9	30.6 ± 4.1	10.4 ± 0.2	3.5 ± 0.1	20.5 ± 2.1
Relative fluorescence unbound[c]	2.10 ± 0.07	3.07 ± 0.12	1 ± 0.01	1.91	2.98	1
Relative fluorescence bound[c]	2.32 ± 0.08	3.07 ± 0.12	1.17 ± 0.04	2.35	2.98	1.24

[a]Mimics $Im7_U$
[b]Mimics $Im7_I$
[c]Normalized to unbound $Im7_N$ or unbound Im7-WT

References:

1. Vogt, A. D. & Di Cera, E. Conformational selection or induced fit? A critical appraisal of the kinetic mechanism. *Biochemistry* **51,** 5894–5902 (2012).

2. Gianni, S., Dogan, J. & Jemth, P. Distinguishing induced fit from conformational selection. *Biophys. Chem.* **189,** 33–39 (2014).

3. Ferguson, N., Capaldi, A. P., James, R., Kleanthous, C. & Radford, S. E. Rapid folding with and without populated intermediates in the homologous four-helix proteins Im7 and Im9. *J. Mol. Biol.* **286,** 1597–1608 (1999).